3.2 COASTAL CURRENTS AND WAVES ALONG THE TEXAS COASTAL BEND: MEASUREMENTS AND MODEL COMPARISONS

Philippe E. Tissot, Larry Dell
Conrad Blucher Institute, Texas A&M University-Corpus Christi, Corpus Christi, Texas

1. INTRODUCTION

Observations and modeling of the movement of water along the coastline of the Gulf of Mexico are important for a broad range of applications including preparation for and response to oil spills, search and rescues, long term planning of coastal infrastructure all contributing to more resilient coastal communities. This proceeding is a follow up to a prior contribution (Tissot et al., 2015) describing the installation and initial measurements from a pair of current profilers and pressure/wave sensors installed near Corpus Christi, Texas. The present contributions expand on the initial results and presents two applications enabled by the data collected.

The two sensors were installed during spring 2014 on the seaward end of Bob Hall Pier, collocated with a National Water Level Observation Network (NWLON 2016) station. The pier is located on the northern end of North Padre Island near two inlets and close to sensitive avian and aquatic habitats. The sensors provide near real-time measurement of nearshore conditions including significant wave height, typical wave period, and average along and cross shore currents as well as horizontal current profiles for both sensors. In addition to the aforementioned applications the resulting data is also applicable for reporting surf conditions, and alerting beach-goers to conditions favorable to the onset of rip currents. The measurements may also be applied to model sediment transport in support of local beach nourishment operations at a nearby popular beach located along North Padre Island.

Measurement and modelling of deep water ocean currents in the Gulf is well documented (e.g. Sturges and Lugo-Fernández, 2005). Near real-time measurements are available for the North West Gulf of Mexico from offshore buoys operated by the Texas Automated Buoy System (TABS) (Guinasso et al., 2009) and several buoys from the National Data Buoy Center (NDBC 2016). Water levels and atmospheric conditions are continuously monitored by stations of the Texas Coastal Ocean Observation Network (Rizzo et al. 2014) and the National Water Level Observation Network (NWLON 2016). However at present there is only one permanent station in the Gulf of Mexico measuring water levels in the nearshore region along the Texas coast. Several other stations measure water level but are protected by ship channel jetties. Also there are presently no other station measuring continuously nearshore ocean currents or wave climate along the Texas open coast.

The information shared in this extended abstract first provides a reminder of the experimental set-up followed by an update of the measurements time series. Correlations between observations and shoreline conditions, mainly alongshore wind, are presented. The article goes on to tackle two applications made possible by this new data set. First a wave history to 2003 is estimated by correlating the measured significant wave heights with the standard deviation of the water levels measured at the collocated NWLON station. The correlation and the challenges of the method are discussed for this location. The significant wave height history is used to estimate wave runup and total water levels leading to estimates of the frequency at which several vertical heights are reached. The concept is referred here as an inundation datum. In the second application nowcasts from three different operational hydrodynamic models are compared to the measurements and the differences discussed. The higher resolution model is then used to explore nearshore circulation along the shores of the Coastal Bend including identifying occasional patterns of stronger nearshore currents.

2. EXPERIMENTAL SET-UP

The sensors installed and maintained for this project are two 2D current profilers, both Xylem (Sontek/YSI) Argonaut SL500 (500 kHz) (Sontek 2009). The instruments were selected, in part, for their range, form factor, narrow beams and experience of the team in deployment and maintenance of this type of equipment. The sensors are installed on the seaward end of a 378 m long pier located along Texas Coastal Bend near Corpus Christi, Texas, Bob Hall Pier (Figure 1). Figures 2 and 3 illustrate the respective locations of the two sensors and the overall experimental geometry. The locations of the sensors and their supporting infrastructure were selected to minimize interaction with fishermen who regularly utilize the pier. In particular, the offshore looking sensor was mounted along one of the piles of the structure supporting the NWLON instrumentation located just behind the T-head. Observations supporting that the experimental geometry

* *Corresponding author address*: Philippe E. Tissot, Texas A&M University-Corpus Christi, Conrad Blucher Institute, 6300 Ocean Drive, Corpus Christi, TX 78412; e-mail: philippe.tissot@tamucc.edu.

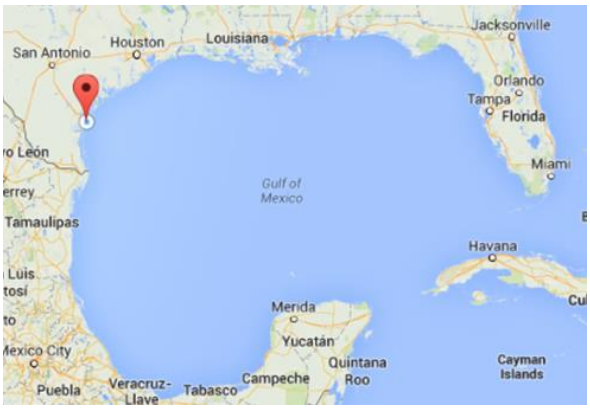

Figure 1. Location of the experiment along the shores of the Coastal Bend in the northwestern part of the Gulf of Mexico.

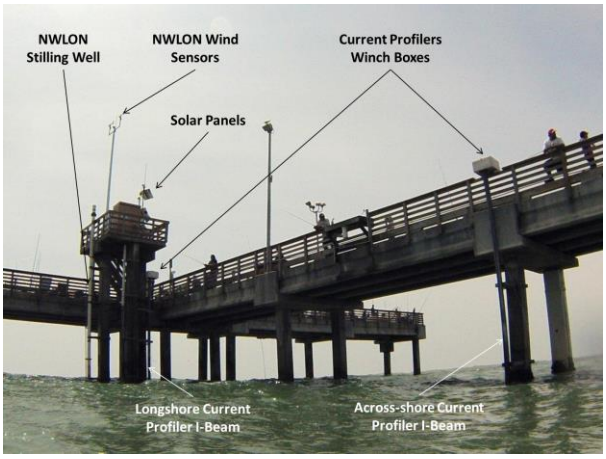

Figure 2. Illustration of the overall experimental geometry with the locations of both the offshore and the nearshore looking current profilers at the seaward end of Bob Hall pier.

and in particular that the current profiler sonic beams straddle the pier piles are discussed in (Tissot et al. 2015) along with more detailed information on the installation and experimental set-up.

The offshore looking sensor is set up to measure current profiles from 10 to 120 m offshore from the sensor in bins of 11 m. The sensor also measures 1024 s time series pressure data leading to the computation of significant wave height and typical wave period. Measurements from the offshore looking sensor are recorded at a 30-min interval. The nearshore looking sensor measures current in narrower bins of 5 m starting 1.5 m away from the instrument and up to 51 m in a direction parallel to the shoreline. Measurements of the nearshore looking sensor are recorded at a 6-min interval. The locations and approximate range of the current profilers are illustrated in Figure 3.

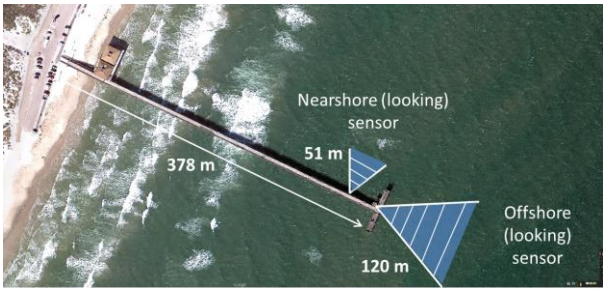

Figure 3. Illustration of the experimental geometry with the locations of the current profilers on the pier and the approximate volumes sampled by each divided in ten bins.

Bob Hall Pier is also home to a permanent station of the NOAA National Water Level Observing Network or NWLON (NOAA 2016b) recording water level and meteorological conditions. The combination of the different sensors provides a great opportunity to study coastal processes along the coast of the Gulf of Mexico, assess the predictions of coastal models and assess and develop new methodologies and guidance for coastal stakeholders.

3. OBSERVATIONS

3.1 Range of Consistent Current Measurements

As described in the previous section both sensors measure current profiles within 10 bins. The offshore looking sensor is set up for a maximum range of 120 m with water conditions, e.g. the amount of particulates in the water, impacting the strength of the reflected signal and the actual useful range. The horizontal profiles or the series of measurements for each of the 10 bins for the signal to noise ratio and the standard error were considered to determine the range of consistent current measurements (Tissot et al, 2015). The distributions were found to be symmetric up to the start of bin 6 coinciding with a distance of 65 m with consistent measurements still observed for bin 6 corresponding to 65-76m but with a substantially higher standard error. Based on this analysis, current measurements are considered up to bin 5 for a year round analysis or a distance of 65 m. Measurements from bins 7 through 10 can still provide useful measurements at time depending on the strength of the backscatter signal with the likelihood of obtaining useful information decreasing with distance.

The measurement consistency at the short end of the offshore looking profiler was also assessed by considering the absolute value of the longshore current profile distributions up to 65 m or bin 5. The current distribution of the first bin clearly indicated slower currents as compared to the bins further away from the sensor and was not considered in the analyses. Slower currents were, in part, attributed to the influence of the pier adjacent to the first bin and possibly related to the

presence of a large migrating sand bar that was identified immediately in front of the pier during sensor installation. Accordingly, bins 2 through 5 are considered reliable for the long term analysis of longshore currents. No significant differences in currents were observed between these 4 current bins and the rest of the analysis presented here is carried out based on currents measured in bin 5 (54-65m).

For the nearshore looking sensor the maximum range of the profile is 51 m, too short to be affected by the decreasing strength of the backscattered signal at that location. As there are no structures in front of the sensor there are no limitations on short range measurements. As the nearshore waters are shallower, limitations for this sensor are associated with large waves and possibly migrating sand bars. The vertical span of the sound beams at the end of the measurement range (51 m) is 3.4 m for the SL 500 and is well contained within the typical water column depth, about 5.5 m at that location. During large wave events the depth of the water column is however periodically reduced leading to interferences with the air water interface at the end of the measurement range, starting with the shoreward beam. Measurements from the near shore looking sensor must therefore be carefully analyzed to avoid including such events.

3.2 General Conditions and Observations

Coastal hydrodynamics along the South Texas coast is influenced by one of the windiest coastal climates in the United States combined with small tidal ranges. Wind distributions are essential to the analysis of longshore currents and coastal processes in general. Winds measured at the collocated NWLON station are used for this study. Figure 4 presents a wind rose for the measured winds during the study period (6/13/2014-12/31/2015). The wind signal is then split between alongshore and cross-shore directions. The wind rose illustrates a predominantly southeasterly onshore flow with stronger northerly winds accompanying the periodic passage of cold fronts from September through April.

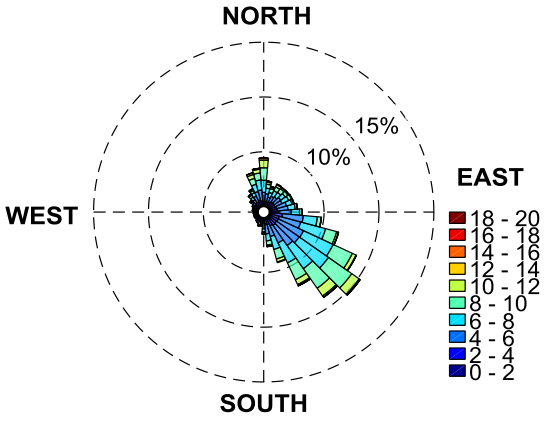

Figure 4. Wind rose for the study period (m/s).

Table 1 presents statistical summaries of the longshore current and wave measurements during the study period. Sensor or communication problems resulted in several gaps spread throughout the study period. Overall during the 18.5 months of the data set, missing current measurements totaled 18.9% of the data with interruptions or periods of sporadic data longer than three days taking place during the following time spans: 8/6-20/14, 11/11-14/2014, 11/25/2014-12/2/2014, 12/29/2014-1/16/2015, 4/2-16/2015, 11/28/2015-12/4/2015 and 12/22-31/2015. Wave data was missing or sporadic during the same time frame. Additionally wave data was removed for the period of 11/4-18/2014 due to a problem with the pressure measurements resulting in a total of 24.3% of the data missing. The longest typical wave period of 11.2s and 11.5s were observed respectively during the influence of Tropical Storm Dolly on September 2, 2014 and the impact of Tropical Storm Bill on June 16, 2015. The largest significant wave heights of 1.8m up to 2.0m were observed during the impact of Tropical Storms Dolly and Bill as well as during high wind events and frontal passages on 9/16/2015, 10/22-23/2015, 11/27-28/2015 and 12/27/2015. Longshore currents were summarized using the 5th bin of each sensor. Both sensors measured longshore currents within a range of about -1.0 m/s and +1.0 m/s, with median longshore currents at or close to 0.0 m/s.

Table 1. Summary of wave and longshore current measurements during the observation period (6/13/2014-12/31/2015).

	Median	**Range**
Wave Measurements		
Significant Wave Height	0.7 m	[0.1m, 2.0 m]
Typical Wave Period	5.9 s	[2.1 s, 11.5 s]
Current Measurements		
Nearshore Longshore Current	0.00 m/s	[-0.9 m/s, 0.8 m/s]
Offshore Longshore Current	-0.03 m/s	[-1.0 m/s, 0.9 m/s]

The wave height distribution during the study period is further illustrated in Figure 5. The measured significant wave heights can be fitted with a Rayleigh distribution with a scale parameter of 0.589 with a 95% confidence interval of [0.586,0.593].

As expected longshore currents measured by both current profilers are strongly correlated to the along shore winds. Computation of these correlation coefficients was updated based on the additional year of data available since the prior publication. The correlations of longshore currents with along shore wind are respectively:

Nearshore longshore current = 0.76
Offshore longshore current = 0.80

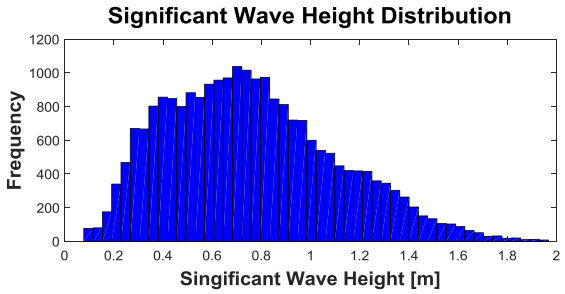

Figure 5. Significant wave height distribution during the study period.

The correlations of longshore currents with significant wave heights are respectively:

Nearshore longshore current = 0.14
Offshore longshore current = 0.10

Other significant correlations include:

Significant wave height and across shore currents for the offshore looking sensor = 0.06
Cross-shore wind & significant wave height = 0.42

p values are negligible (<0.0) given the now extensive length of the data sets with over 20,000 measurements for all time series.

4. NOWCASTING AND HINDCASTING OF WAVE HEIGHTS

Wave heights can be estimated based on the standard deviation of the water levels if measured at a nearby location (Parker 1991, Park et al. 2014, NOAA 2014). For this study water levels are measured at the collocated Corpus Christi NWLON station making it a good match location wise. The modeling approach is to fit a linear regression between the two time series. For this location, and likely other locations, the process is complicated by variability in the range of the water level standard deviation. Obstructions of the stilling well or its connected parallel plates at the bottom of the well can further dampen the amplitude of the water level variability in the tube. While this should not affect the measurement of average water levels the standard deviation is affected. For the present location the standard deviation of water levels was downloaded (Rizzo et al., 2014) for the two year period of 1/1/2015 through 12/31/2015. After graphical investigation of the time series, the data was divided into three distinct periods with significant differences in mean and standard deviations as presented below. The means and standard deviations are also compared with the 13 year period of 2003 through 2015. Note that no data was collected between 4/30/2015 and 6/8/2015.

(1) 1/1/2014-6/15/2014 mean = 0.009 m (0.008)
(2) 6/15/2014-4/30/2015 mean = 0.092 m (0.043)
(3) 6/8/2015-12/31/2015 mean = 0.137 m (0.071)
(4) 1/1/2003-12/31/2015 mean = 0.072 m (0.070)

The standard deviation during period (1) was clearly dampened and inconsistent with the long term mean of the water level standard deviation. The second period from 6/15/2014 through 4/30/2015 was the closest to the long term mean and selected for this study. A scatter plot illustrates the relationship between the water level standard deviation and the significant wave height for this time period. The theoretical expression for the relationship between the two variables is swh = 4*sigma (NOAA, 2014). Also small and small waves could be removed such constraints were not imposed in this case in large part to obtain a better fit for most of the data set and the larger wave range of particular interest for this study.

Significant Wave Height ~= 6.704 x standard deviation of water levels + 0.1046. {1}

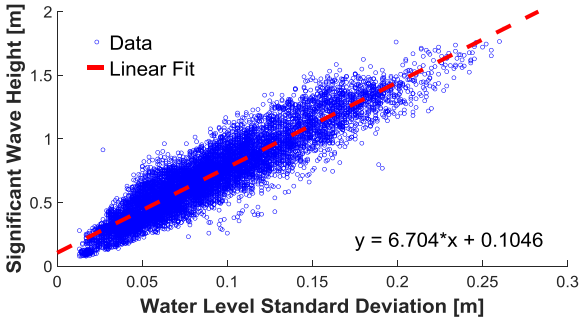

Figure 6. Scatter plot of significant wave heights vs water level standard deviation with illustration of the linear regression.

Model residuals are presented in Figure 7 showing relatively little bias and with a standard deviation of 0.12 m.

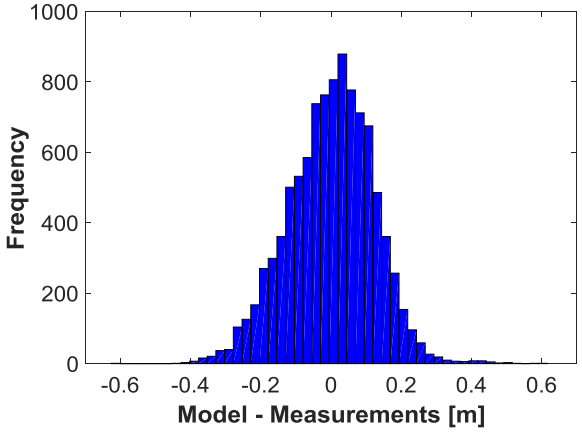

Figure 7. Residual distribution for the significant wave height model during the period of 6/15/2014-4/30/2015.

The results above are good with little sign of a nonlinear relationship known to affect the acoustic protective well

depending on wave height, wave period, and water depth (Shih and Rogers, 1981) except for wave heights smaller than about 0.3m.

While the results above are quite good for this portion of the data set, a different relationship would have been obtained if the linear fit had been computed for the period of 6/8/2015-12/31/2015 with a linear coefficient of 4.42. With both periods combined the linear coefficient would have been 4.61. The curve fit for the period of 6/15/2014-4/30/2015 was retained for the next step as its mean was closest to the overall 13 year data set. This variability is in part likely caused by obstructions of the bottom of the well where the parallel plates are mounted to reduce pull down effects.

Given the variability of the relationship between the water level standard deviation and the significant wave height measurements, the following portion of this study is a conceptual demonstration of what can be achieved with the derived relationship above. For more accurate results further data processing beyond the scope of this contribution should be undertaken to remove portion of the water level standard deviation history inconsistent with the calibration or long term variability. Given these limitations equation (1) was applied to the period 2013-15. The resulting wave history is presented in Figure 8.

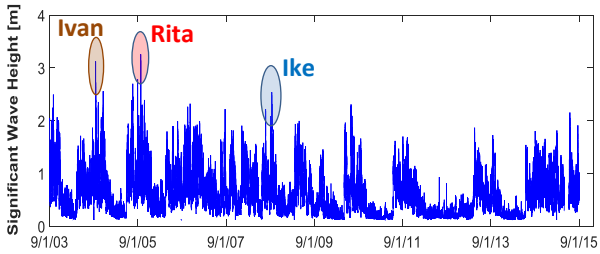

Figure 8. Reconstructed wave height history for Bob Hall Pier with identification of the hurricanes which impact included the highest wave events on record.

The wave reconstruction allows to identify with realistic wave heights past hurricanes that have impacted the Coastal Bend. Figure 8 also highlights periods of unrealistically long low wave activity likely due to dampening of the signal in the stilling well as discussed above.

The combination of measured still water levels at the NWLON station with estimated significant wave height based on the standard deviation of water levels at the same location allows fo an estimate of wave run up. Based on a set of experiments performed at the USACE SUPERTANK, Roberts et al. (2010) found that the vertical extent of wave runup was approximately equal to the significant breaking wave height. In the present context the wave run-up or vertical reach of the water was similarly estimated by summing up the measured still water and the estimated significant wave height. This resulted in a time series (2003-2015) of vertical reach of the water along the beach. Based on this data the frequency with which water reaches the station's tidal datums was computed. Tidal datums are computed based on still water levels at the tide gauge and hence filter out most of the wave effect. When adding the wave contribution, a tidal datum such as Mean Sea Level is expected to be submerged far more frequently than its name may imply. The estimated inundation frequencies or frequency with which the water reaches to its vertical height is illustrated in Figure 9 for several tidal datums: Highest Astronomical Tide (HAT), Mean Higher High Water (MHHW), Mean Sea Level (MSL) and Mean Lower Low Water (MLLW). In this estimate water reaches the HAT level about 50% of the time. This type of statistics could be helpful for beach managers.

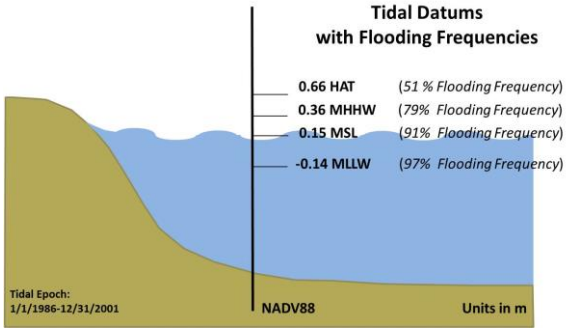

Figure 9. Illustration for Bob Hall Pier (Corpus Christi) tidal datums with their respective estimated flooding frequency.

While tidal datums can be accurately computed and are important for multiple purpose such as establishing legal littoral boundaries, the frequency at which water reaches a vertical location on the beach is more relevant when planning beach maintenance or the location of structures. The vertical heights along the beach corresponding to 5%, 10%, 30% and 50% flooding frequencies were estimated based on the same data set. The results are illustrated in Figure 10. These estimates are akin to an inundation datum that can be estimated when both significant wave height and still water levels are available for a location.

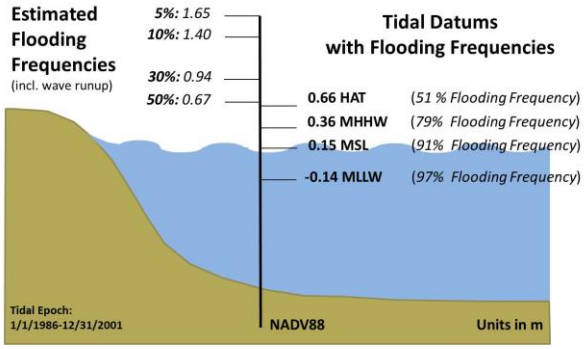

Figure 10. Illustration for Bob Hall Pier (Corpus Christi) of a proposed Inundation Frequency diagram to complement tidal datums.

As coastal decision makers will increasingly be required to make decisions impacted by relative sea level rise, visualization of tidal datums and estimated inundation frequencies on could further help the planning of beach maintenance and infrastructure location. An example is presented in Figure 11. A benchmark that is part of the NWLON station network of benchmark is located on top of the illustrated pier pile. Based on this benchmark, tidal datums and inundation datums are illustrated along the same pier pile.

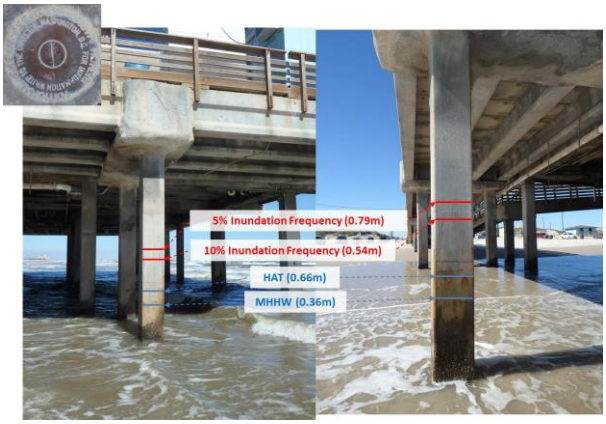

Figure 11. Illustration of the inundation frequency datums on one of the Bob Hall Pier (Corpus Christi) piles. The use of locally recognized landmark facilitates communication of the concept.

5. COMPARISON WITH OPERATIONAL CURRENT NOWCASTS: NGOFS/ROMS/HYCOM

This data set of nearshore current observations is also an occasion to assess the performance of operational models for the location. Data from three operational models were downloaded for their respective grid cell containing the location of the sensors. In addition data from the further offshore buoy TABS D (TABS, 2016) were downloaded for further comparison. Water current predictions were downloaded for the initial state of the water current forecast, or time zero predictions for the following models:

- The Northern Gulf of Mexico Operational Forecast System (NGOFS) (Wei et al. 2014), built using the Finite-Volume Coastal Ocean Model (FVCOM, Chen et al., 2003), is an unstructured three-dimensional primitive equation based hydrodynamic model. Resolution ranges from 10 km offshore to 600 meters close to shore. NGOFS generates water level, current, temperature and salinity nowcasts and forecasts four times per day. The National Oceanic and Atmospheric Administration (NOAA) built and maintains NGOFS. The locations of the Bob Hall Pier and TABS D locations relative to the NGOFS grid are illustrated in Figure 12 while the location of the project sensors relative to the NGOFS grid is illustrated in Figure 13 (NGOFS element # 50649). As part of the model discussion and documentation Wei et al. (Wei et al., 2014 & NOAA, 2015) assessed the NGOFS performance based on four parameters: water level, current velocity, temperature and salinity measured at 72 stationary stations within the model grid. The reader is referred to these publications for a broad assessment of the model performance. The present assessment is location and application specific.
- The ROMS or Regional Ocean Model System (ROMS) is a free-surface, hydrostatic, primitive equation ocean model that uses stretched, terrain-following coordinates in the vertical and orthogonal curvilinear coordinates in the horizontal. TAMU built and maintains the General Land Office (GLO) ROMS Hydro Model for the Gulf of Mexico. Resolution varies from about 33 km offshore to about 4.4 km onshore. The resolution in the Coastal bend including around Bob Hall Pier and the TABS D buoy is about 4.8 km. More information on ROMS can be found at myroms.org. The GLO Hydrodynamic Model uses ROMS and covers the entire Gulf of Mexico. Archived files can be found at: http://csanady.tamu.edu/GNOME/gnome2-cat.html#GROM_hind_reg_sfc_24.
- The Hybrid Coordinate Ocean Model (HYCOM) implementation in the Gulf of Mexico is based on a squared ~3.5 km horizontal grid. For its vertical grid HYCOM has an isopycnic-coordinate system in the deep stratified regions of the model and depth following sigma layers in shallower coastal waters. The transition between coordinate types is dynamic in space and time. The model has 40 vertical layers. When retrieving coastal predictions data for three layers are made available for three layers with the surface layer spanning 0 to 5m. More information on HYCOM can be found here: https://hycom.org/hycom/overview. The Navy is in charge for the upkeep of HYCOM.

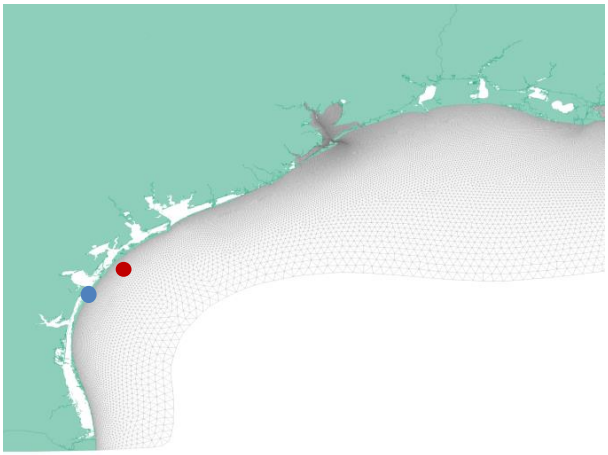

Figure 12. Illustration of the western portion of the NGOFS grid (NOAA 2016c) with the Bob Hall Pier (blue dot) and TABS D (red dot) sensor locations indicated.

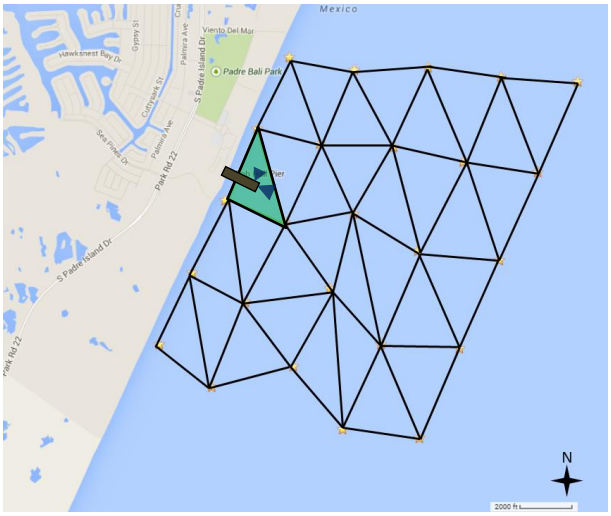

Figure 13. Location of the NGOFS grid element (element # 50649) corresponding to the project sensor location on Bob Hall Pier, Texas.

For the BHP location, longshore current measurements from the offshore looking sensor are compared with each of the models upper layer current predictions. Results are illustrated in the scatter plots of Figure 14. For the NGOFS the first sigma layer represents 2.5% of the location water depth or about 0-0.15m. For the ROMS model the surface layer represents 5% of the water column or about 0-0.3m. For the HYCOM model shoreline cells have a depth of 5m and hence the predictions are akin to depth averaged predictions over most of the water column.

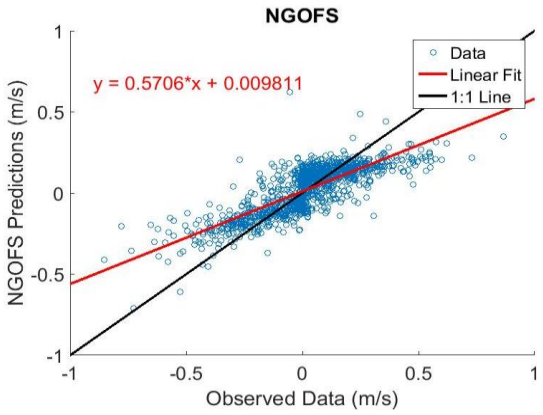

(a)

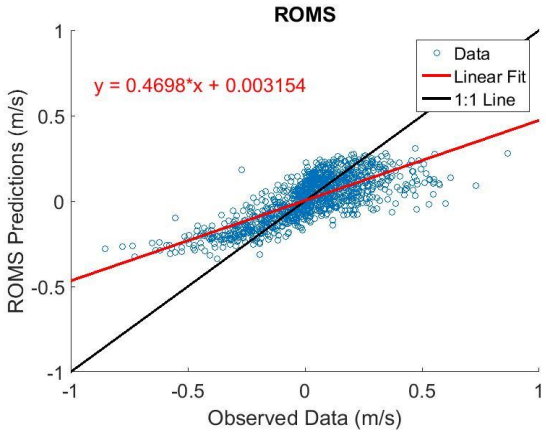

(b)

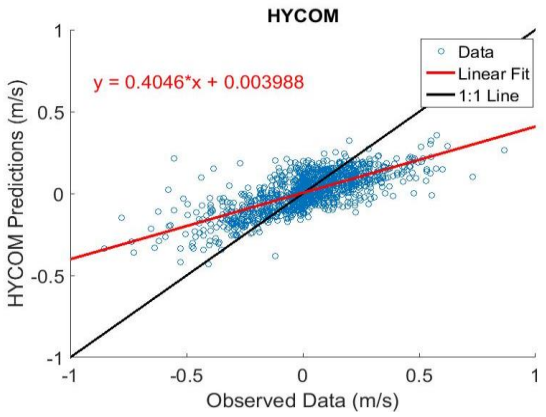

(c)

Figure 14. Scatter plots of predicted currents (upper layer predictions) with currents measured at the study location.

The statistical performance metrics presented in Table 2, including RMSE and CF, were selected based on NOAA's standards for evaluating operational nowcast and forecast hydrodynamic model systems (Hess et al., 2003). The Central Frequency for current predictions quantifies the percentage of the predictions that are within 26 cm/s.

As illustrated in Figure 14 the relationship between predicted and measured longshore currents is consistent throughout the observed range for all three models. The model predictions all underestimate measurements at the Bob Hall Pier locations but the comparisons are for somewhat different currents. For all models, the predictions represent averaged values over their respective grid cells while the measurements are for a specific location just seaward of Bob Hall Pier. The location is relatively central with respect to the NGOFS grid cell while on the nearshore side of the ROMS and HYCOM grid cells. Also the measurements are depth averaged while the predictions vertical spans vary. The

Table 2. Summary of wave and longshore current measurements during the observation period (6/13/2014-12/31/2015).

Model	RMSE (m/s)	Bias (m/s)	CF (<0.26 m/s)
Bob Hall Pier Comparisons			
NGOFS (surface 0-0.15m)	0.13	0.00	95.0%
ROMS (surface 0-0.3m)	0.14	-0.01	93.4%
HYCOM (0-5m)	0.15	-0.01	91.5%
TABS D Comparisons			
NGOFS	0.16	0.09	91.4%
ROMS	0.19	-0.04	82.7%
HYCOM	0.20	0.11	84.4%

NGOFS and ROMS longshore surface current predictions are typically stronger than depth averaged predictions due to the increasing impact of bottom friction while moving towards the ocean floor. Hence comparing surface predictions with volume averaged measurements should have led to larger predicted currents. However all three models under predict the observed currents with predicted currents respectively about 57%, 47% and 40% of the observed currents for the observation period. This reinforces the assessment that hydrodynamic models underestimate longshore current at the study location with the caveat that these are not direct comparisons. Model performance is further compared in Table 2. The somewhat lower performance of the HYCOM predictions was expected as depth averaged predictions will have smaller predicted current speeds and hence will further under predict the location's longshore current.

For the NGOFS model measurements are further compared with depth average predictions but for a different time frame. At a distance of 54m-65m from the sensor the vertical beam spread is about 4m. NGOFS predictions were averaged for layers 8-33 or about 1.1-5.1m for a water depth of 6.2m to better reflect the vertical extent of the sensor's measurement range. The prediction/measurements comparison was assessed over the one year period of 1/1/2015 through 12/31/2015. The difference between the depth average current predictions and the measurements was a little larger than the comparison with the surface current predictions: RMSE of 0.12 m/s, Bias of -0.01 m/s, and CF(0.26 cm/s) of 95.1% for the depth averaged predictions as compared to a RMSE of 0.12 m/s, Bias of -0.00 m/s, and CF of 96.0% for the surface predictions. The slopes of scatter plots similar to the data presented in Figure 14 yielded values of 0.60 for the surface predictions and as expected a lower value of 0.52 for the depth averaged predictions. The small difference in performance of the NGOFS model over year 2015 as compared to the time frame used in Table 2 (6/13/2014-12/31/2015) is attributed to seasonal effects. The comparison between NGOFS surface and depths averaged predictions gives a quantitative estimate of the relatively small difference between the two predictions. The difference would be substantially larger if the depth average included layers close to the ocean floor but this lower portion of the water column is not measured by the sensor.

The respective model performances were also compared with TABS D measurements. The NGOFS and HYCOM models underpredict surface currents while no substantial under or over prediction is observed for ROMS (Dell et al., 2015). The overall performance for all models and both locations is presented in Table 2. All models provide skillful predictions with somewhat lower rms and higher CF for NGOFS possibly related to its higher resolution and focus on the coast. The difference are however not sufficient to conclude that one model is clearly better than another model for predictions at the coastal location of Bob Hall Pier, Texas. In the next section output from the NGOFS model is used in part because of its good performance but mainly for its higher coastal resolution.

6. IDENTIFICATION AND DESCRIPTION OF A COASTAL CURRENT FEATURE ALONG THE TEXAS COASTAL BEND

Given the good agreement between current measurements and model predictions at the Bob Hall Pier and TABS-D locations, the gridded output of the NGOFS model was further used to characterize typical spatial surface current distributions for the study area. The comparison was conducted to help quantify and characterize differences between offshore predictions and nearshore predictions observed at times by responders. Nearshore surface current patterns are particularly important for oil spill response and search and rescue operations. Gridded surface current nowcasts were downloaded for the study area for the period 12/1/2014 through 11/30/2015. Quiver plots were generated for each surface current map. Surface current patterns were further identified and characterized using a self-organizing map (SOM) neural network (MATLAB, 2015). SOM neural networks were previously used by Liu and Weisberg (Liu, 2005) to characterize currents along the West Florida Shelf. Surface current predictions were analyzed for the 27.4° through 28.0° N and 96.7° through 97.6° W area. Use of three clusters was found to be the optimal number to delineate current patterns in the area. Only current vector data was used in the algorithm to avoid biases from location and bathymetry during clustering.

On recurring occasions a narrow band with higher shoreline currents as compared to further offshore currents was identified. On other occasions shoreline currents were predicted to be in a different direction as compared to further offshore locations. An illustration of

a narrow stronger shoreline current feature is presented in Figure 15.

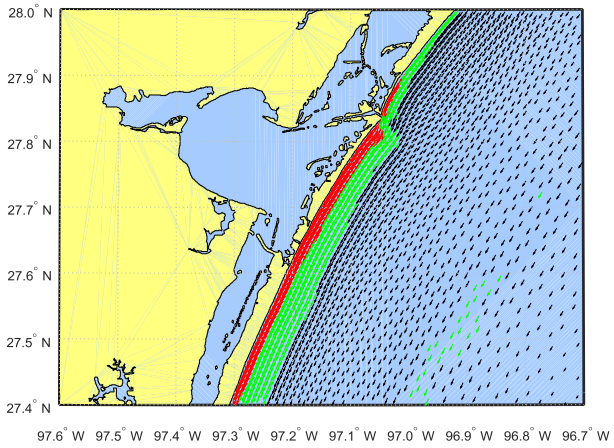

Figure 15. Predicted surface currents for the Coastal Bend for January 8, 2015 03:00 UTC. Areas of similar currents are identified with a self-organizing map algorithm including the identification of a narrow shoreline area of higher longshore currents.

To identify more systematically occurrences of shoreline currents substantially different than further offshore currents surface current profiles offshore of Bob Hall Pier were further investigated. An example of a current profile is presented in Figure 16. The following criteria and the following criteria were selected:

1. Difference of maximum predicted nearshore currents (0-2.3km) and minimum further offshore predicted currents (2.5-21.7km) > 0.14 m/s
2. A narrow shoreline feature identified in the predicted surface current map by the SOM algorithm.

While a difference of 0.14m/s may not seem large, such longshore current difference translates to 12.1km per day. A times series of the max/min current differences is further illustrated in figure 17. A total of 88 events were identified based on the surface current differences with 70 of these events or 80% retained after further consideration of the surface current maps and the results of the SOM algorithm. Additional cases of surface current maps with significantly different shoreline currents are presented in Figures 18 and 19.

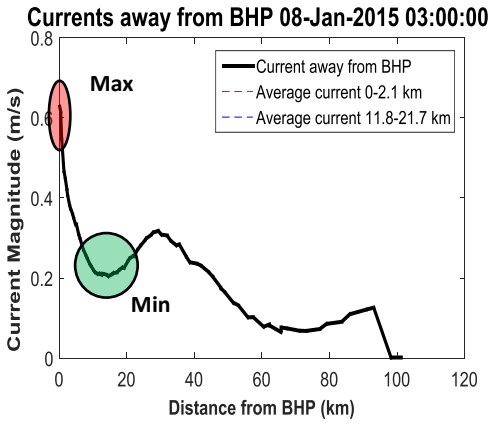

Figure 16. Predicted surface current profile offshore of the Bob Hall Pier location for January 8, 2015, 0300 UTC. The nearshore maximum current and further offshore minimum current are illustrated.

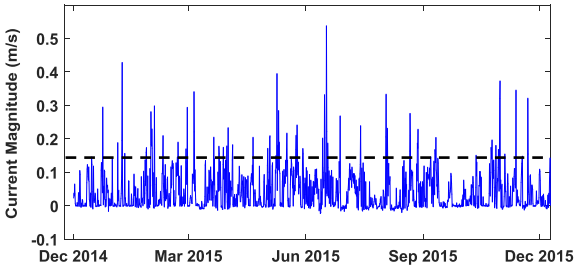

Figure 17. Illustration of the time series of the difference between maximum predicted nearshore currents and minimum further offshore predicted currents with the selected 0.14 m/s limit.

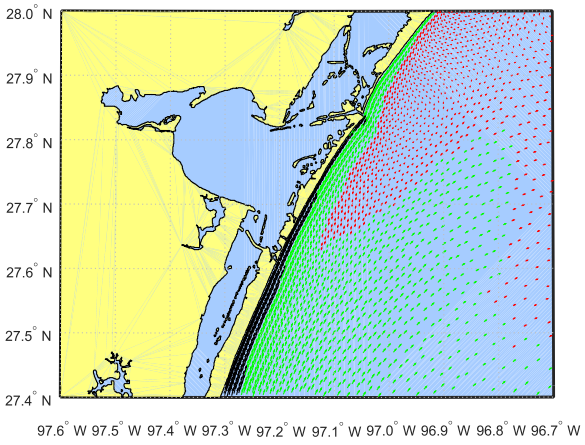

Figure 18. Predicted surface currents for the Coastal Bend for October 31, 2015 03:00 UTC. Areas of similar currents are identified with a self-organizing map algorithm including the identification of a narrow shoreline area of higher longshore currents.

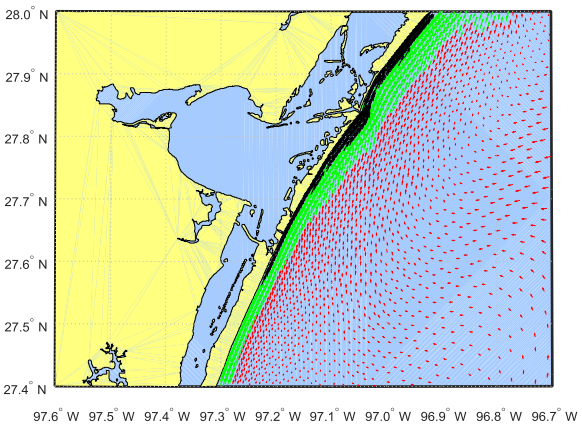

Figure 19. Predicted surface currents for the Coastal Bend for June 17, 2015 03:00 UTC. Areas of similar currents are identified with a self-organizing map algorithm including the identification of a narrow shoreline area of higher longshore currents.

The difference between nearshore and further offshore currents during these 70 events are further quantified in Table 3 at the end of this proceeding. The 70 events represent about 5% of the surface current patterns for 12/1/2014 through 11/30/2015. Three different types of conditions lead to these nearshore/further offshore surface current differences including frontal passages (20) and strong southeasterly winds (7). The majority of the cases took place during conditions leading to current reversals (43) with the nearshore surface flow in the opposite direction of further offshore currents. The median nearshore current feature widths were about 10km wide with a range of 1.8-26km. The median predicted peak shoreline currents are strongest for the frontal passage periods (0.41 m/s) as compared to the strong southeasterly periods (0.29 m/s) and the reversal periods (0.22 m/s). The corresponding minimum further offshore currents are 0.15 m/s, 0.08 m/s and 0.03 m/s respectively. In all cases the median differences between nearshore and further offshore currents are substantially larger than the 0.14 m/s criterion, 0.26 m/s for the frontal passages and around 0.20 m/s for the other cases. While median peak winds ahead of the cases are high (9 – 12 m/s) the sole presence of high winds does not in general lead to the onset of a these nearshore current features.

It should be reminded that the current patterns discussed here are model output and not measurements. Given the good performance of the NGOFS model for the two verification locations this discussion should still provide good guidance for coastal stakeholders for the type of differences that can be expected between shoreline and further offshore currents. Better guidance could be obtained if instrumentation such as HF Radar observations were permanently available along the coast.

7. DATA ACCESS

Wave and longshore current measurements along with water levels, air and water temperature and wind information are accessible through a website formatted for smartphone users. The page (see Figure 20) is accessible at http://cbi-apps.tamucc.edu/bhpwave/. The latest atmospheric conditions and water level measurements are obtained from the collocated NWLON station.

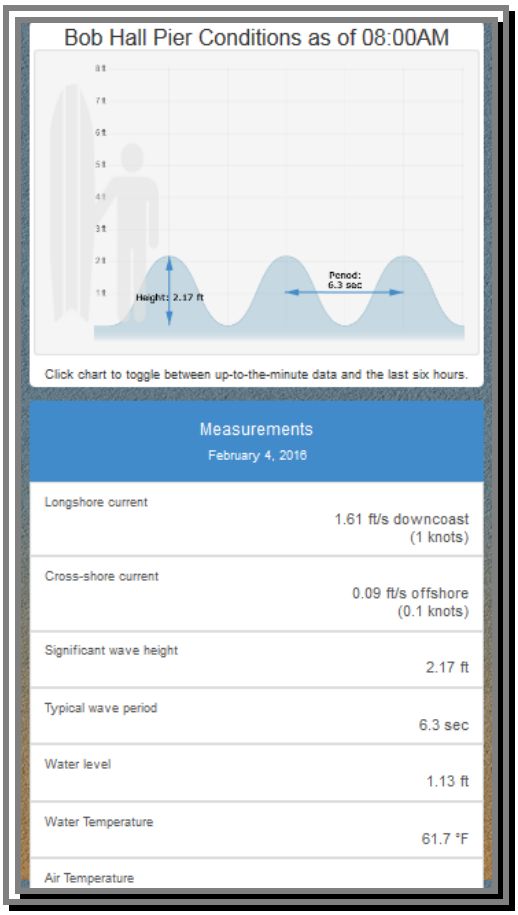

Figure 20. Example of display of conditions with the website optimized for smartphone display at the sensors location.

Project data can also be accessed through the Conrad Blucher Institute website at the following station webpages:

Offshore looking sensor:
http://www.cbi.tamucc.edu/obs/260

Nearshore looking sensor:
http://www.cbi.tamucc.edu/obs/259

For the offshore looking sensor, Velocity X displays the longshore current with a positive current indicating a south-southeast direction. Velocity Y corresponds to the cross shore current with a positive current indicating an

offshore direction. For the nearshore looking sensor, Velocity X corresponds to the cross shore current with positive values indicating an offshore current. Velocity Y with positive values indicates a longshore current in the North-Northwest direction.

8. DISCUSSION & CONCLUSIONS

Two current profilers and wave sensors were installed during spring 2014 on a pier located on the open coast near Corpus Christi, Texas. One of the sensors is oriented to monitor conditions offshore of the pier while the other sensor is positioned to measure profiles in a direction parallel to the shoreline.

Measurements during the study period (6/13/2014-12/31/2015) yielded significant wave heights ranging from 0.1 to 2.0 m and typical wave periods between 2.1 and 11.5 s. Longshore currents measured by both sensors, one offshore of the last sand bar and the other typically inside of this last bar, were both in a range of about -1.0 to 1.0 cm/s. The strongest currents, the largest significant waves and the longest typical wave periods were associated with the landing of Tropical Storms Dolly and Tropical Storm Bill as well as a few high wind events and frontal passages.

The time series of measured significant wave heights was correlated with the standard deviation of the water levels measured at the collocated NWLON station. A relationship was used to hindcast a significant wave height history for the location back to 2003. With the estimate that runup can be approximated by the significant breaking wave height a history of total water levels was hindcast for the location. The data was then used to estimate the inundation frequencies of tidal datums emphasizing that even the Mean Higher High Water Level or Highest Astronomical Tide datums are under water more than 50% of the time due to wave run up and atmospheric forcings. It is argued that inundation datums could be helpful to complement tidal datums for coastal managers when making practical decisions related to what portion of the nearshore stays dry.

The collected data was further used to quantify the differences between measurements and predictions for three operational hydrodynamic models: NGOFS, ROMS and HYCOM. While taking into account that the measurements are for a specific location while the model predictions are averaged over a grid cell, and that measured and predicted depth spans are different model predictions were found to be consistent for the observation range. The rmse varied from 0.13 m/s to 0.15 m/s and CF(0.26 m/s) from 91.5% to 95.0% for the Bob Hall Pier location. The respective model performances were also compared for the further offshore buoy of TABS D. The rmse varied from 0.16 m/s to 0.20 m/s and CF(0.26 m/s) from 82.7% to 91.4% for that location. All models under predicted observations for the Bob Hall Pier location with predicted currents ranging from 40% to 60% of the observed currents for the three models. The NGOFS and HYCOM models under predicted surface currents while no substantial under or over prediction was observed for ROMS at that location. CF(0.26 m/s) vary from 84.4% to 91.4% for that location.

Given its good performance for both the Bob Hall Pier and TABS-D locations, the gridded output of the NGOFS model was further used to characterize typical surface current patterns in the study area. On recurring occasions a narrow band with higher shoreline currents as compared to further offshore currents was identified. On other occasions shoreline currents were predicted to be in a different direction as compared to further offshore locations. The nearshore current feature was associated with frontal passages, strong southeasterly winds and current reversals. The median width of the feature is approximately 10km with median current differences between the nearshore and further offshore estimated at 0.26 m/s for frontal passages and about 0.20 m/s for the other two cases. These types of events were observed for about 5% of the predicted current maps. Such observation even if based on modeled data is helpful for coastal stakeholders and is consistent with prior observations from oil spill responders that led to this study.

Observations are continuing at the study location with considerations for additional collocated instrumentation to create a more complete data set including optics based method to map surface currents and study the onset of rip currents.

9. ACKNOWLEGEMENTS

Funding for the work presented in this paper was provided by Nueces County Parks and as part of a R&D 2014-2015 Funding Cycle grant from the Texas General Land Office (TGLO). Both are gratefully acknowledged. The views expressed herein are those of the authors and do not necessarily reflect the views of TGLO or Nueces County.

The authors also wish to acknowledge members of the Conrad Blucher Institute field crew and information technology teams for efficiently and creatively resolving problems throughout the project. Finally Anthony Reisinger is gratefully acknowledged for participating to and making one of the field trips possible.

10. REFERENCES

Cox, D.T., P.E. Tissot, and P. R. Michaud, 2002a: Water Level Observations and Short-Term Predictions Including Meteorological Events for the Entrance of Galveston Bay, Texas. *J. of Wtwy, Port, Coast., and Oc. Engrg.*, 128-1, 21-29.

Liu, Y. and Weisberg, R.H. (2005) Patterns of Ocean Current Variability on the West Florida Shelf Using the Self-Organizing Map. J. Geophysical Res., 110(C06003), 1-12.

The MathWorks, Inc., 2014: *Neural Network Toolbox*, *Matlab R2014a*. The MathWorks, Natick, MA.

NDBC, cited 2016: Western Gulf of Mexico Recent Marine Data [Available online at http://www.ndbc.noaa.gov/maps/WestGulf.shtml.]

NOAA, cited 2016a: Bob Hall Pier, Corpus Christi, TX – Station ID: 8775870 [Available online at http://tidesandcurrents.noaa.gov/stationhome.html?id=8775870.]

NOAA, cited 2016b: The National Water Level Observation Network (NWLON) [Available online at http://tidesandcurrents.noaa.gov/nwlon.html]

NOAA, cited 2016c: The Northern Gulf of Mexico Operational Forecast System (NGOFS) [Available online at https://tidesandcurrents.noaa.gov/ofs/ngofs/ngofs_info.html]

NOAA, 2015: *NOAA Technical Report NOS CS 35*: The Nested Northwest and Northeast Gulf of Mexico Operational Forecast Systems (NWGOFS and NEGOFS): Model Development and Hindcast Skill Assessment. National Oceanic and Atmospheric Administration, Silver Spring, Maryland.

NOAA, 2014: *NOAA Technical Report NOS CO-OPS 075*: Water level and Wave Height Estimates at NOAA Tide Stations from Acoustic and Microwave Sensors. National Oceanic and Atmospheric Administration, Silver Spring, Maryland.

NOAA, 1994: *NOAA Technical Memorandum NOS OES 8*. National Oceanic and Atmospheric Administration, Silver Spring, Maryland.

Park, J. R. Heitsenrether and W. Sweet, 2014: Water Level and Wave Height Estimates at NOAA Tide Stations from Acoustic and Microwave Sensors. *J. Atmos. Oceanic Technol.*, 31(10), 2294-2308, doi: 10.1175/JTECH-D-14-00021.1.

Parker, B., 1991: Tidal Hydrodynamics. Wiley, 912 pp.

Rizzo, J., P. Tissot and S. Duff (2014): The Texas Coastal Ocean Observation Network. *Proc. of Oceans' 14*, September 15-18, St. Johns, Newfoundland, CA. Institute of Electrical and Electronics Engineers, doi 10.1109/OCEANS.2014.7003131.

Roberts, T. M. Roberts, P. Wang, and N. C. Kraus, 2010: Limits of Wave Runup and Corresponding Beach-Profile Change from Large-Scale Laboratory Data. *J. Coastal Research:* vol. 26 (1), 184 – 198.

Simoniello, C., P. Tissot, D. McKee, D., A. Adams, R. Ball and R. A. Butler, R. A., 2010: Cooperative Approach to Resource Management: Texas Gamefish Win. *J. Marine Technology Society*, vol.44 (5), pp5-9, doi http://dx.doi.org/10.4031/MTSJ.44.5.5.

Smith, N.P., 1980: Temporal and Spatial Variability in the Longshore Motion Along the Texas Gulf Coast. J. Geophysical Res., 85(C3), 1531-1536.

SonTek, 2009: Argonaut-SL System Manual Firmware Version 12.0. SonTek/YSI, San Diego, California, 316 pp. [Available online at ftp://rrcs-173-196-209-21.west.biz.rr.com/pub/outgoing/Argonaut-SL.pdf.]

MATLAB, 2015, MATLAB R2015a, The MathWorks Inc., Natick, MA, 2000.

Tissot, P.E., D.T. Cox, A. Sadovski, P. Michaud and S. Duff, 2004: Performance and Comparison of Water Level Forecasting Models for the Texas Ports and Waterways. *Proc. of the PORTS 2004 Conference*, Houston, TX, Amer. Soc. Civil Engineers [Available online at http://ascelibrary.org/doi/abs/10.1061/40727%282004%29129.]

Tissot, P.E., D.T. Cox, and P.R. Michaud, 2003: Optimization and Performance of a Neural Network Model Forecasting Water Levels for the Corpus Christi, Texas, Estuary. *Proc. of the 3rd Conference on the Applications of Artificial Intelligence to Environmental Science*, Long Beach, California, February 2003.

Tissot, P., L. Dell, J. Rizzo, D. Williams (2015) Nearshore Measurements of Wave Climate and Current Profiles along the Texas Coastal Bend. Proceedings of the 13th Symposium on the Coastal Environment, AMS 95th Annual Meeting. [Available online at https://ams.confex.com/ams/95Annual/webprogram/Paper269560.html].

Wei, E., Z. Yang, Y. Chen, J.G.W. Kelley, A. Zhang, 2014: The Northern Gulf Of Mexico Operational Forecast System (NGOFS): Model Development and Skill Assessment. NOAA Technical Report NOS CS 33, 190pp. [Available online at http://www.nauticalcharts.noaa.gov/csdl/publications/TR_NOS_CS33_FY_14_02_Eugene_NGOFS_report.pdf.]

Wei, E.; Zhang, A.; Yang, Z.; Chen, Y.; Kelley, J.G.; Aikman, F.; Cao, D. (2014): NOAA's Nested Northern Gulf of Mexico Operational Forecast Systems Development. *J. Mar. Sci. Eng.* 2014, *2*, 1-17.

Table 3. Summary of the observed wind measurements and predicted currents during the identified higher shoreline current events for the observation period (6/13/2014-12/31/2015).

Conditions	Number of Cases	Median Prior Peak Wind (Direction)	Median Shoreline Feature Width (Range)	Median Peak Shoreline Current (Location Range)	Median Minimum Current
Frontal Passages	20	12 m/s (10°)	9.1 km (3.1–16 km)	0.41 m s^{-1} (0.9<3.9 km)	0.15 m s^{-1}
Strong Southeasterlies	7	10 m/s (150°)	11.8 km (7.5-26 km)	0.29 m s^{-1} (1.0<4.2 km)	0.08 m s^{-1}
Current Reversals	43	9 m/s (130°)	11.8 (1.8-24 km)	0.22 m s^{-1} (1.4 <6.8 km)	0.03 m s^{-1}